

Support Vector Machine Model for Diagnosing Pneumoconiosis Based on Wavelet Texture Features of Digital Chest Radiographs

Biyun Zhu · Hui Chen · Budong Chen · Yan Xu · Kuan Zhang

Published online: 9 July 2013
© Society for Imaging Informatics in Medicine 2013

Abstract This study aims to explore the classification ability of decision trees (DTs) and support vector machines (SVMs) to discriminate between the digital chest radiographs (DRs) of pneumoconiosis patients and control subjects. Twenty-eight wavelet-based energy texture features were calculated at the lung fields on DRs of 85 healthy controls and 40 patients with stage I and stage II pneumoconiosis. DTs with algorithm C5.0 and SVMs with four different kernels were trained by samples with two combinations of the texture features to classify a DR as of a healthy subject or of a patient with pneumoconiosis. All of the models were developed with fivefold cross-validation, and the final performances of each model were compared by the area under receiver operating characteristic (ROC) curve. For both SVM (with a radial basis function kernel) and DT (with algorithm C5.0), areas under ROC curves (AUCs) were 0.94 ± 0.02 and 0.86 ± 0.04 ($P=0.02$) when using the full feature set and 0.95 ± 0.02 and 0.88 ± 0.04 ($P=0.05$) when using the selected feature set, respectively. When built on the selected texture features, the SVM with a polynomial kernel showed a higher diagnostic performance with an AUC value of 0.97 ± 0.02 than SVMs with a linear kernel, a radial basis function kernel and a sigmoid kernel with AUC values of 0.96 ± 0.02 ($P=0.37$), 0.95 ± 0.02 ($P=0.24$), and 0.90 ± 0.03 ($P=0.01$), respectively. The SVM model with a polynomial kernel built on the selected feature set showed the highest diagnostic performance among all tested models when using either all the wavelet texture features or the selected ones.

The model has a good potential in diagnosing pneumoconiosis based on digital chest radiographs.

Keywords Pneumoconiosis · Classification · Wavelet transform · Texture feature · Decision tree · Support vector machine

Introduction

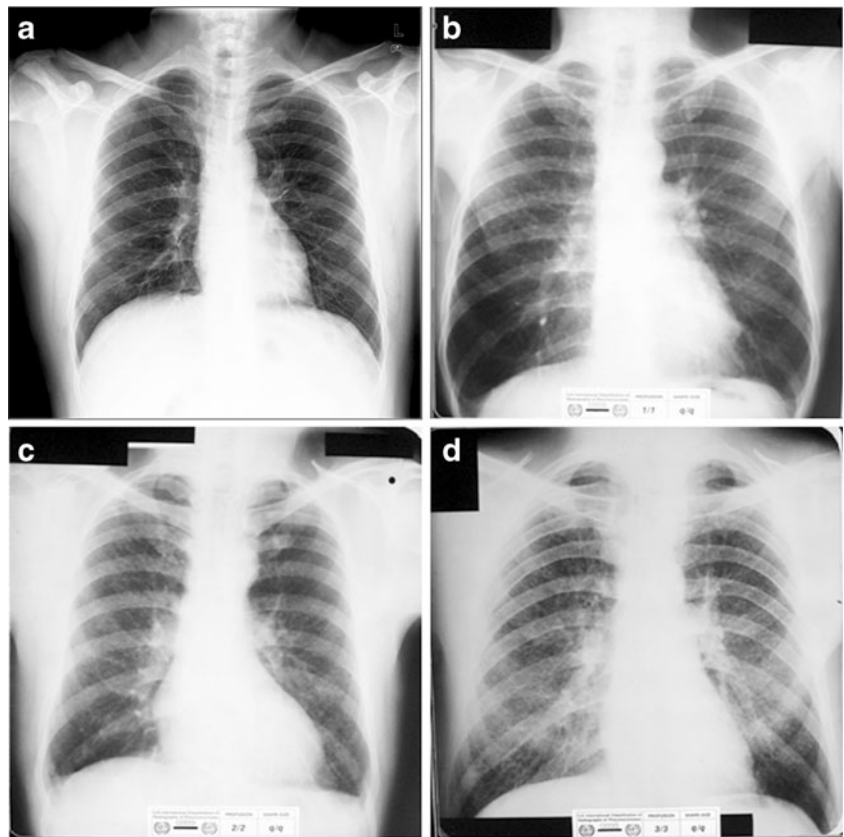
Pneumoconiosis is a major occupational disease caused by inhaled particles, such as free silica, asbestos, mixed dust, and coal. For mass screening of pneumoconiosis, chest radiograph (digital chest radiograph at present) is a prevalent approach; therefore, the International Labor Organization (ILO) established a standardized system for classifying radiographic abnormalities of pneumoconiosis according to the profusion level of small opacities on chest radiographs [1]. Four ILO standard radiographs of normal person and patients with stage I, II, and III pneumoconiosis are shown in Fig. 1. There are only a few small opacities that can be seen from Fig. 1b, c, which make it an error-prone and difficult process for radiologists to distinguish the chest radiographs of a normal person from those of patients with pneumoconiosis, especially from patients with stage I and II pneumoconiosis. Therefore, many investigators devoted themselves to developing computer-aided diagnosis (CAD) schemes which were necessary to reduce the workload and improve the workflow in mass chest screening for pneumoconiosis.

Studies investigating CAD for pneumoconiosis date back to the 1970s, with a recent revival of interest in the late 1990s [2, 3]. Yu et al. [4] detected pneumoconiosis using the gray-level histogram features and the co-occurrence matrices features on digital radiographs (DRs). Their support vector machine (SVM)-based models gave an overall accuracy of up to 89.2 % and an area under the receiver operating characteristic (ROC) curve of up to 0.978 when tested on 300 normal DRs and 125 pneumoconiosis DRs. Using a similar approach, Xu

B. Zhu · H. Chen (✉) · K. Zhang
School of Biomedical Engineering, Capital Medical University,
No. 10 Xitoutiao, YouAnMen, Fengtai District, Beijing 100069,
China
e-mail: chenhui@ccmu.edu.cn

B. Chen · Y. Xu
Department of Radiology, Beijing Friendship Hospital,
Capital Medical University, Beijing 100053, China

Fig. 1 Standard chest radiographs used for the diagnosis of pneumoconiosis. **a** Chest radiograph of a normal person. **b** Chest radiograph of a patient with stage I pneumoconiosis. **c** Chest radiograph of a patient with stage II pneumoconiosis. **d** Chest radiograph of a patient with stage III pneumoconiosis



et al. [5] distinguished 175 pneumoconiosis DRs from 252 normal DRs, giving a 95.5 % overall accuracy. In another investigation [6], power spectra of chest DRs which implied image texture were obtained through Fourier analysis and were input into an artificial neural network with the back-propagation algorithm to detect pneumoconiosis, resulting in an area under ROC curve (AUC) of 0.961. In our previous study [7], the use of texture features extracted through gray-level histogram and co-occurrence matrix of chest DRs and artificial neural network with the back-propagation algorithm also suggested a relatively high performance for the diagnosis of pneumoconiosis.

Generally, the performance of machine learning classifiers depends on many factors, such as the classification models and their structure or parameter settings, the training methods, the datasets, and the selected features [8]. In this paper, we focused on the investigation of the impact that the classification models and the input features put on the performance of the classifiers when they were used to diagnose pneumoconiosis based on DRs. We used the wavelet transform-based texture features of chest radiographs, which to our best knowledge have never been used in previous studies of CAD schemes for pneumoconiosis, as the classifiers' input features. Classification models chosen in this study were the decision tree (DT) and the SVM. The performances of the classifiers with different parameter

settings as well as the classifiers built on different feature sets were then compared and discussed.

Materials and Methods

Study Dataset

A total of 125 DRs collected from the Beijing Friendship Hospital were analyzed in this study. These DRs were 85 posterior–anterior digital chest radiographs for male normal subjects of average age of 62 years old and 40 for male pneumoconiosis patients of stage I and II (20 for each stage) of average age of 61 years old, respectively. All of the images were digitized with a matrix of $2,900 \times 3,000$ and 15-bit gray level in the Digital Imaging Communications in Medicine format. The work was approved by the Beijing Friendship Hospital Research Ethics Committee.

Lung Segmentation

The method for lung segmentation used in this study was based on the traditional Otsu threshold method and was improved by reprocessing the image with a morphological reconstruction filter, which was applied to the original DR to

eliminate local gray-level extremes before the Otsu threshold method was used. The whole image was then partitioned into several connected regions, the contours of which were extracted and smoothened by using connected-components labeling technique and a morphological closing operator. The inside areas of the complete contour with the longest perimeter was segmented as lung fields [9] (as shown in Fig. 2).

Feature Extraction

In medical images, the quantitative or qualitative changes of the texture characteristics often reflect pathological changes. Therefore, many researchers try to analyze various medical images by means of texture analysis to explore new ways for the diagnosis and treatment of some diseases. However, due to the complexity of medical image and their texture features, there is no universal texture analysis method that is suitable for all kinds of medical images.

More recently, methods based on multi-resolution or multi-channel analyses such as the wavelet transform have received considerable attention. After wavelet transformation, the energy of the original image focuses on several wavelet coefficients, which have a high degree of local relevance in detail components of three directions. It provides a favorable condition for feature extraction.

Discrete Wavelets Transform

Compared with the normal DRs, there are a number of small opacities in the pneumoconiosis DRs, resulting in the differences of texture features between the normal and pneumoconiosis DRs. It is a hint that the diagnosis of pneumoconiosis could be conducted by using texture features derived from DRs of lung fields after a series of wavelet transformation.

The two-dimensional wavelet decomposition has two structures: pyramid decomposition and tree structure decomposition. In this paper, the tree structure decomposition was

adopted. After decomposition for the first scale, the original image is divided into four sub-bands, which could be expressed by combinations of L and H (as shown in Fig. 3a). The sub-band LL1 represents the low-frequency sub-image, corresponding to an approximation image, while the sub-bands LH1, HL1, and HH1, collectively called high-frequency sub-images, corresponded to the detail images. For future decomposition, the sub-band LL1 alone is decomposed, resulting in a two-scale wavelet decomposition (as shown in Fig. 3b) [10].

Taking the resolution of the given images used in our study into consideration, each DR image has been wavelet-decomposed for seven times (called a seven-scale wavelet transform), resulting in 28 sub-bands of each image (i.e., LL1, LH1, HL1, HH1...LL7, LH7, HL7, HH7).

Feature Calculation

Energy is a commonly used texture feature in the texture analysis, and it was adopted in our study. In the seven-scale wavelet transform for each DR image, the energy E_{kl} for the l th sub-band image at the k th scale ($l = 1$ to 4 and $k = 1$ to 7, respectively) is calculated as follows [11]:

$$E_{kl} = \frac{1}{M_k \cdot N_k} \sum_{i=1}^{M_k} \sum_{j=1}^{N_k} x(i, j)^2 \quad (1)$$

where M_k and N_k represent the size of sub-band images at the k th scale (the four sub-band images at the k th scale are of equal size as $M_k \times N_k$) and $x(i, j)$ ($i = 1$ to M_k and $j = 1$ to N_k , respectively) is the gray value of pixel (i, j) of the image. The final feature vector contains 28 energy features of wavelet coefficients calculated in sub-bands at successive scales.

Since the order of magnitude, ranging from 10^{-1} to 10^4 , differed quite a bit among these features in this study, the pre-processing of these features was necessary in order to provide informative data for the classifier. Logarithmic transformation was applied to the feature values before they were input into the classifiers.

Fig. 2 Results of lung field segmentation. **a** Original digital chest radiograph of a patient with stage I pneumoconiosis. **b** Segmented lung fields from the original digital chest radiograph with the background in black

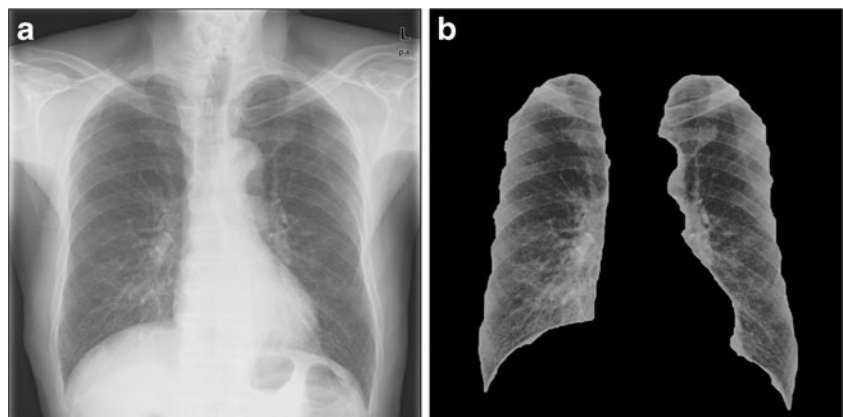
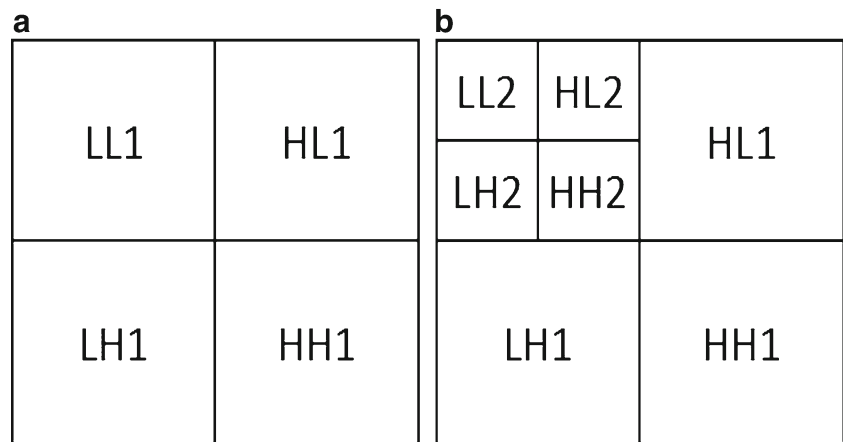


Fig. 3 Sketch map of the discrete wavelet transform on a 2D image. **a** After the first-scale wavelet transform on the whole image, it was divided into four sub-bands, namely, LL1, LH1, HL1, and HH1. **b** After the second-scale wavelet transform on sub-band LL1, it was divided into four sub-bands, namely, LL2, LH2, HL2, and HH2. Here *H* and *L* denote the high- and low-pass filters, respectively



Classification Models

There are many available models for binary classification, such as DT, Bayesian networks, SVM, and neural networks. Two popular, but not being used, models in our study scenario, DT and SVM, were selected to perform the classification.

Decision Tree

Decision trees are powerful classification algorithms that are becoming more and more popular with the growth of data mining methods. A DT-based classifier is expressed as a DT or a set of if-then rules, forms that are generally easier to understand than neural networks. The common DT algorithms include ID3, C4.5, C5.0, the classification and regression tree, and the chi-square automatic interaction detector. Essentially, DT is a process of data classification on the basis of a series of splitting criteria, among which three of the most well-known splitting criteria are based on the Gini index, entropy, and the chi-square test [12, 13].

Of all the DTs, DT with algorithm C5.0 can handle numeric attributes and can induce from a training set that incorporates missing values by using corrected gain ratio criteria [14]. The splitting ceases when the number of instances to be split is below a certain threshold. Error-based pruning is performed after the growing phase. Due to its applicability and interpretability, DT with algorithm C5.0 was selected as one of the classifiers in our study.

Support Vector Machine

The SVM, put forward by V.N. Vapnik et al., is a research direction of statistics, which is developed based on small sample data and has a strong ability of generalization to high-dimension space. For the binary class issue, the basic idea for SVM is to construct a hyperplane that maximizes the margin between negative and positive examples. The classification performance of SVM is closely related to the choice of

kernel function, which is used to construct the hyperplane and the relevant parameter settings for every kernel function. There are many kinds of kernel functions used for SVMs. However, there is no uniform standard to judge the suitability of the kernel function for a particular application [15, 16], and there is no standard guidance for the selection of parameters. In this study, the following four kernels were selected for further comparisons, and the parameter settings depended on experience:

$$\text{Linear kernel } K(x, y) = x \cdot y \tag{2}$$

$$\text{Polynomial kernel } K(x \cdot y) = (x \cdot y + 1)^q, q = 1, 2, \dots, N \tag{3}$$

$$\text{Radial basis function (RBF) kernel } K(x, y) = \exp\left\{-\frac{\|x - y\|^2}{2\sigma^2}\right\} \tag{4}$$

$$\text{Sigmoid kernel } K(x, y) = \tanh[v(x \cdot y) + c] \tag{5}$$

Model Validation and Performance Assessment

Model Validation

In this study, *k*-fold cross-validation was used to assess the classification models. In *k*-fold cross-validation, the complete data set is randomly split into *k* mutually exclusive subsets of approximately equal size. The classification model is trained and tested *k* times. At each time, it is trained on all folds but one and tested on the remaining single fold [17].

Due to the relatively small sample size in this study, *k* was selected as 5. By stratified sampling, all of the 125 DR samples were randomly divided into five folds, including 17 normal and eight pneumoconiosis DRs for each fold. At each modeling-validating iteration, four folds of samples

containing 68 normal cases and 32 abnormal cases were used to build the classifier models, and the remaining fold of samples containing 17 normal cases and eight abnormal cases was used to assess the performance of the classifiers.

Performance Assessment and Comparison

Accuracy, sensitivity (the percentage of pneumoconiosis DRs being correctly classified as abnormal), and specificity (the percentage of normal DRs being correctly classified as normal) were used as objective measures to assess the classification performance. The ROC curve analysis was used to further evaluate and compare the performance of two classifiers. An ROC curve is a graphic plot in which the values of sensitivity are plotted on the *Y* axis and those of one minus specificity are plotted on the *X* axis for a binary classifier system, and the area under the ROC curve (AUC) is used as a single measure for evaluation and comparison. ROCKIT software (Charles E. Metz, Department of Radiology, University of Chicago, USA) was employed for the ROC curve analysis.

Results

Training and Setting Classification Models

For an SVM with a particular kernel, the soft margin parameter *C* which was used to penalize the decision errors when searching for the maximum marginal hyperplane was determined experimentally as 10. Other parameters for the training process were as follows: (1) the tolerant error for stopping the training was set at 0.001 and (2) the parameter epsilon of the insensitive loss function was set at 0.1.

The parameters of each SVM kernel were set by trial and error. They were (1) $q = 3$ for the polynomial kernel in Eq. (3), (2) $\sigma^2 = 0.1$ for the RBF kernel in Eq. (4), and (3) $c = -1$ and $\nu(z)$ for sigmoid kernel in Eq. (5).

Performance of Both Classifiers with Different Feature Sets

A total of 28 energy features of wavelet coefficients were calculated in the 28 sub-bands, namely the full feature set. Upon the full feature set, a DT with algorithm C5.0 and an SVM with an RBF kernel were built to discriminate normal DRs from pneumoconiosis ones, respectively. After the five-fold cross-validation, the classification performances were obtained. In terms of accuracy, sensitivity, specificity, and AUC value (listed in Table 1), the SVM all showed a higher performance than the DT.

When building the DT model, not all of the features were retained in the model, which means that some of the features were redundant and were removed from the full feature set automatically by the DT algorithm. According to the results of

Table 1 Performance of the decision tree with algorithm C5.0 and of the support vector machine with radial basis function kernel for the diagnosis of pneumoconiosis by using different feature sets

Classification model	Feature set	Performance index			
		Accuracy (%)	Sensitivity (%)	Specificity (%)	AUC value
DT	Full	83.2	70.0	89.4	0.86
	Selected	88.0	82.5	90.6	0.88
SVM	Full	87.2	80.0	90.6	0.94
	Selected	88.8	80.0	92.9	0.95

DT decision tree, SVM support vector machine, AUC area under ROC curve

Pearson correlation analysis on each pair of all the features, features that had a high correlation (i.e., the correlation coefficient was greater than 0.95) with at least one of the features retained in the DT model were selected. The selected features and those retained in the DT model composed the selected feature set, which contained 16 features out of the full feature set. The performance of the DT and of the SVM, which were built on the selected feature set, is also listed in Table 1, respectively.

The ROC curves for SVMs and DTs built on both full feature set and the selected feature set are shown in Fig. 4.

As the results indicated, the classification performances were improved in terms of the accuracy and the AUC value for both the DT and SVM with the selected feature set compared to those with the full feature set. Furthermore, on the selected feature set, the AUC value for the SVM was 0.95 ± 0.02 . It was greater than that for the DT (0.88 ± 0.04),

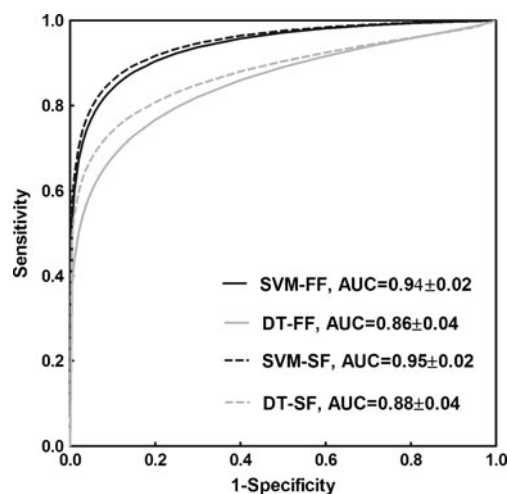


Fig. 4 Comparison of receiver operating characteristic curves for decision tree (DT) models with algorithm C5.0 and support vector machine (SVM) models with radial basis function kernel for the diagnosis of pneumoconiosis. SVM-FF SVM model with the full feature set, DT-FF DT model with the full feature set, SVM-SF SVM model with the selected feature set, DT-SF DT model with the selected feature set

showing that the SVM had a superior performance to the DT for the detection of pneumoconiosis on DRs.

Performance of SVMs with Different Kernels

Accuracies, sensitivities, specificities, and AUC values of SVMs built on the selected feature set with different kernels when diagnosing pneumoconiosis based on DRs are listed in Table 2. ROC curves of these SVMs are shown in Fig. 5. The SVM model with a polynomial kernel showed a higher diagnostic performance in terms of AUC value than SVMs with a RBF kernel ($P=0.24$), a linear kernel ($P=0.37$), and a sigmoid kernel ($P=0.01$), respectively.

Discussion

Several computerized schemes have been developed for the detection and classification of pneumoconiosis on chest radiographs. Some studies [2, 18, 19] detected the small rounded or somewhat irregular opacities on a chest radiograph and then classified the radiograph as a normal radiograph or a pneumoconiosis one according to the standardized system for classifying radiographic abnormalities of pneumoconiosis as established by the International Labor Organization. Other studies [3–5, 20] took the texture analysis on the chest radiographs to diagnose pneumoconiosis. Texture features used in these studies included statistical texture features from the gray-level histogram and gray-level co-occurrence matrix, power spectrum, and frequency on the chest radiographs. Diagnostic models built in these studies showed different performances due to the different methods and dataset. Theoretically and practically, the performance of classifiers depends on many critical factors, such as the database used, the features extracted and selected, the classifier chosen, and even the validation method when evaluating the system performance [8].

Table 2 Performance of the support vector machines with different kernels for the diagnosis of pneumoconiosis by using the selected feature set

SVM kernel	Performance index			
	Accuracy (%)	Sensitivity (%)	Specificity (%)	AUC value
Polynomial	92.0	82.5	96.5	0.97
Linear	88.8	87.5	89.4	0.96
Radial basis function	88.8	80.0	93.0	0.95
Sigmoid	84.8	77.5	87.1	0.90

SVM support vector machine, AUC area under ROC curve

Dataset of Digital Chest Radiographs

In clinical practice, it is relatively not too hard for radiologists to make a diagnostic decision on pneumoconiosis of stage III based on DRs (Fig. 1). However, almost all of the developed computerized schemes were built and tested on sample DRs that included pneumoconiosis DRs of stage III. To build and evaluate a more clinically meaningful model for the diagnosis of pneumoconiosis, DR samples of patients with stage III pneumoconiosis were excluded from our study. With only DRs of patients with stage I and II pneumoconiosis and of normal individuals, the SVM classifier built in this work got a rather high performance with an accuracy of up to 92.0 % and an AUC value of up to 0.97, which was not inferior to or even superior to those developed by using DR samples including DRs of stage III pneumoconiosis in other studies [4, 6].

Feature Extraction and Selection

Texture analysis on the chest radiographs proved to be helpful when diagnosing lung diseases and breast diseases [21, 22]. Texture features had been used by many investigators in developing computerized schemes for pneumoconiosis [3, 4, 6, 7, 16, 17]. However, traditional statistical texture features may have some disadvantages when applied to digital chest radiographs [23], such as the huge computation. More recently, methods based on multi-resolution or multi-channel analysis, such as Gabor filters and wavelet transform, have received a great deal of attention. The wavelet transform provides a precise and unifying framework for the analysis and characterization of a signal at different scales

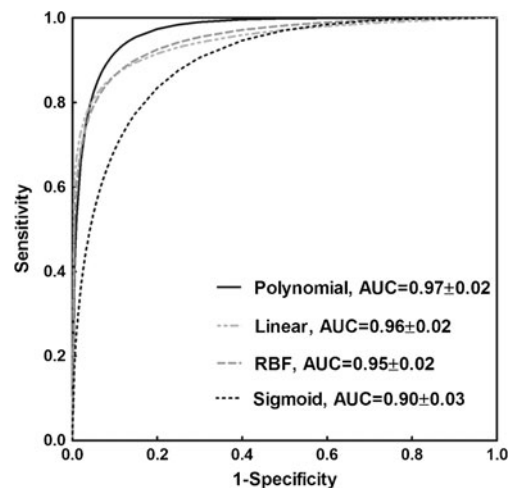


Fig. 5 Comparison of receiver operating characteristic curves for the support vector machines with different kernels which were built on the 16 selected features out of 28 energy features. The area under the curve (AUC) for the polynomial kernel SVM is greater than those for SVMs of linear kernel, radial basis function kernel, and sigmoid kernel ($P=0.37$, 0.24 , and 0.01 , respectively)

[10]. In this paper, we tried using the energy of wavelet coefficients as the texture features to build classification models for the diagnostic tasks. Based on 28 energy features extracted after seven successive scales of wavelet transform, an SVM classifier presented a higher performance compared to our previous one [7] with an accuracy of 87.2 % and an AUC value of 0.94.

Furthermore, considering that redundant or irrelevant features may affect the performance of classification models [24], we conducted a feature selection by using the correlation analysis in alignment with the DT model. The resulting feature set included 16 selected features out of the total of 28 features. With the selected feature set, performances of the SVM- and DT-based classifiers were both improved (Fig. 4; Table 1). The experimental results suggested that the wavelet texture features of DRs were feasible and helpful in diagnosing pneumoconiosis.

Classifiers and Their Parameter Settings

DTs and SVMs are two popular machine learning models for application in binary classification. The DT is considered as easy to interpret, whereas SVM has a relatively poor interpretability. That is, compared to SVM, one can understand more easily why a DT classifies an instance as belonging to a specific class. However, the advantages of an SVM are notable. It is more suitable to learning tasks where the number of features is large with respect to the number of training samples, and SVM tends to perform much better when dealing with multiple dimensions and continuous features [25, 26]. Some studies [27–29] showed that SVMs had better classification efficiency than DTs. In our study, the two models were chosen for pneumoconiosis diagnosis using DR images. By means of a five-fold cross-validation, SVMs outperformed DTs on the basis of both the full feature set and the selected feature set in terms of accuracy and AUC value (Fig. 4; Table 1). The result was similar to those derived from the cited studies.

For the SVMs, it is well known that there are no golden rules for determining which kernel will result in the most accurate one. Some researchers believed that the kernel chosen did not generally make a large difference in resulting accuracy [30]. In this study, a further comparison of classification performances of SVMs with four different kernels (as listed in Eqs. (2), (3), (4), and (5)) was conducted. The SVM with a polynomial kernel showed the highest performance among the four SVMs (Fig. 5; Table 2), especially compared to the SVM with a sigmoid kernel ($P=0.01$), which was equivalent to a simple two-layer neural network known as a multilayer perception. Of course, the results were just obtained under our study condition and there is still no universal conclusion

regarding the performance comparison of SVM models with different kernels.

Other Influence Factors

For a classifier that built on the texture features extracted from a segmented image area, the classification results may be affected by the segmentation accuracy. To investigate the influence of segmentation accuracy, we randomly selected nine DRs of three normal subjects, of three patients with stage I pneumoconiosis, and of three patients with stage II pneumoconiosis. Lung fields of these DRs were segmented automatically by the algorithm presented in this paper and manually by an experienced thoracic radiologist, respectively. There was little difference among the wavelet energy features calculated on these image areas, resulting in few influences on the classification results. The reasons may lie in that the small opacities accumulated mainly inside the lung fields that may cause little change of the texture features. Another reason may be that the shortage of the edges due to the inaccuracy segmentation just occupied a small fraction of the whole lung fields, which led to less effect on the classification result.

In addition, the results were obtained from a relatively limited number of cases (85 normal cases and 40 cases of pneumoconiosis) in this study. For sample size calculation for SVMs, some simulation studies revealed that the relative performance of the different combinations of classifier and feature selection method depends on the feature space distributions, the dimensionality, and the available training sample sizes [31, 32]. SVM is an effective classifier for the problems of high dimension and small sample sets; however, the finite-sized available sample may still introduce variance and bias into the performance of the trained classifier relative to that obtained with an infinite sample size and further have an adverse impact on generalization and robustness of the trained classifier. Therefore, the classifier models could benefit from a larger size of samples.

Conclusions

When used to differentiate between normal and pneumoconiosis chest radiographs based on the wavelet transform-based energy texture features, the SVM model with a polynomial kernel built on the selected feature set showed the highest performance among all of the tested models when using either the full feature set or the selected feature set. The model has a good potential in diagnosing pneumoconiosis based on digital chest radiographs.

Acknowledgments This work was partially supported by the Science and Technology Project of Beijing Municipal Education Commission, China (No. KM201110025008). The authors are grateful to Dr. Haiying Quan for the helpful suggestions.

References

1. International Labor Organization (ILO): Guidelines for the use of the ILO international classification of radiographs of pneumoconiosis. Occupational Safety and Health Series, No. 22 (Rev.). International Labor Office, Geneva Switzerland, 1980.
2. Savol AM, Li CC, Hoy RJ: Computer-aided recognition of small rounded pneumoconiosis opacities in chest X-rays. *IEEE Trans Pattern Anal Mach Intell* 2:479–482, 1980
3. Hall EL, Crawford WO, Roberts FE: Computer classification of pneumoconiosis from radiographs of coal workers. *IEEE Trans Biomed Eng* 22:518–527, 1975
4. Yu P, Xu H, Zhu Y, Yang C, Sun X, Zhao J, et al: An automatic computer-aided detection scheme for pneumoconiosis on digital chest radiographs. *J Digit Imaging* 24:382–393, 2011
5. Xu H, Tao X, Sundararajan R, et al.: Computer aided detection for pneumoconiosis screening on digital chest radiographs. *Proc. Third International Workshop on Pulmonary Image Analysis*, 129–138, 2010.
6. Okumura E, Kawashita I, Ishida T: Computerized analysis of pneumoconiosis in digital chest radiography: effect of artificial neural network trained with power spectra. *J Digit Imaging* 24:1126–1132, 2011
7. Cai C, Zhu B, Chen H: Computer-aided diagnosis for pneumoconiosis based on texture analysis on digital chest radiographs. *Proceedings of International Conference on Electronic, Communication and Computer Science*. Guilin, China, 2012 June 15–17.
8. Chen H, Zhang J, Xu Y, Chen B, Zhang K: Performance comparison of artificial neural network and logistic regression model for differentiating lung nodules on CT scans. *Expert Syst Appl* 39:11503–11509, 2012
9. Zhu B, Chen H: Morphological reconstruction based segmentation of lung fields on digital radiographs. *Proceedings of International Conference on Electronic, Communication and Computer Science*. Guilin, China, 2012 June 15–17.
10. Arivazhagan S, Ganesan L: Texture segmentation using wavelet transform. *Pattern Recogn Lett* 24:3197–3203, 2003
11. Kociołek M, Materka A, Strzelecki M, Szczypiński P: Discrete wavelet transform-derived features for digital image texture analysis. *Proceedings of International Conference on Signals and Electronic Systems*. Lodz, Poland, 2001 September 18–21.
12. Quinlan JR: Induction decision tree. *Mach Learn* 1:81–106, 1986
13. Li C, Zhi X, Ma J, Cui Z, Zhu Z, Zhang C, et al: Performance comparison between logistic regression, decision trees, and multi-layer perceptron in predicting peripheral neuropathy in type 2 diabetes mellitus. *Chin Med J (Engl)* 125:851–857, 2012
14. Maimon O, Rokach L: *Data Mining and Knowledge Discovery Handbook*, 2nd edition. Springer, New York, 2010
15. Zhu Y, Tan Y, Hua Y, Wang M, Zhang G, Zhang J: Feature selection and performance evaluation of support vector machine (SVM)-based classifier for differentiating benign and malignant pulmonary nodules by computed tomography. *J Digit Imaging* 23:51–65, 2010
16. Shawe-Taylor J, Cristianini N: *Kernel Methods for Pattern Analysis*. Cambridge University Press, Cambridge, 2004
17. Olson DL, Delen D: *Advanced Data Mining Techniques*. Springer, LLC, Berlin, 2008
18. Kondo H, Zhao B, Mino M: Automated quantitative analysis for pneumoconiosis. *Proceedings of International Symposium on Multispectral Image Processing*. Wuhan, China, 1998 Oct 21–23.
19. Chen X, Toriwaki J, Hasegawa J: Automated classification of pneumoconiosis radiographs based on recognition of small rounded opacities. *Syst Comput Jpn* 21:33–44, 1990
20. Murray V, Pattichis MS, Davis H, Barriga ES, Soliz P: Multiscale AM-FM analysis of pneumoconiosis x-ray images. *Proceedings of IEEE International Conference on Image Processing*. Kochi, India, 2009 Nov 7–10.
21. Delen D, Walker G, Kadam A: Predicting breast cancer survivability: a comparison of three data mining methods. *Artif Intell Med* 34:113–127, 2005
22. McLaren CE, Chen WP, Nie K, Su MY: Prediction of malignant breast lesions from MRI features: a comparison of artificial neural network and logistic regression techniques. *Acad Radiol* 16:842–851, 2009
23. Mohamed MM, Abdel-Galil TK, Salama MA, El-Saadany EF, Kamel M, Fenster A, Downey DB, Rizkalla K: Prostate cancer diagnosis based on Gabor filter texture segmentation of ultrasound image. *Proc IEEE Can Conf Electr Comput Eng* 3:1485–1488, 2003
24. Bárbara B, Pineda-Bautista JA, Carrasco-Ochoa J, Fco Martínez-Trinidad: General framework for class-specific feature selection. *Expert Syst Appl* 38:10018–10024, 2011
25. Hastie T, Tibshirani R, Friedman J: *The Elements of Statistical Learning*, 2nd edition. Springer, New York, 2009
26. Lim T, Loh W, Shih Y: A comparison of prediction accuracy, complexity, and training time of thirty-three old and new classification algorithms. *Mach Learn* 40:203–228, 2000
27. Elangovan M, Sugumaran V, Ramachandran KI, Ravikumar S: Effect of SVM kernel functions on classification of vibration signals of a single point cutting tool. *Expert Syst Appl* 38:15202–15207, 2011
28. Islam T, Rico-Ramirez MA, Han D, Srivastava PK: Artificial intelligence techniques for clutter identification with polarimetric radar signatures. *Atmos Res* 109:95–113, 2012
29. Marjanovic M, Kovacevic M, Bajat B, Vozenilek V: Landslide susceptibility assessment using SVM machine learning algorithm. *Eng Geol* 123:225–234, 2011
30. Han J, Kamber M: *Data Mining: Concepts and Techniques*, 2nd edition. Elsevier, Maryland Heights, 2006
31. Way TW, Sahiner B, Hadjiiski LM, Chan HP: Effect of finite sample size on feature selection and classification: a simulation study. *Med Phys* 37:907–920, 2010
32. Sahiner B, Chan HP, Hadjiiski L: Classifier performance prediction for computer-aided diagnosis using a limited dataset. *Med Phys* 35:1559–1570, 2008